

# Synthesis and Characterization of Liquid Crystalline Silsesquioxanes

Chunxin Zhang,<sup>†</sup> Timothy J. Bunning,<sup>‡</sup> and Richard M. Laine<sup>\*,†</sup>

Departments of Chemistry, Materials Science and Engineering, and the Macromolecular Science and Engineering Center, University of Michigan, Ann Arbor, Michigan 48109-2136, and Air Force Research Laboratory, Materials and Manufacturing Directorate/MLPJ, Wright-Patterson Air Force Base, Ohio 45433

Received January 19, 2001. Revised Manuscript Received June 1, 2001

With the goal of developing diverse building blocks for nanocomposite materials, we have now learned to synthesize liquid crystalline materials by appending mesogenic groups to cubic silsesquioxane cores (LC cubes) via hydrosilylation of allyloxy functionalized mesogens (**4**, **5**, **8**, and **9**) with octakis(dimethylsiloxy)octasilsesquioxane ( $Q_8M_8^H$ ). On average, hydrosilylation leads to cubes with an average of five LC groups attached, which differ from the more “regular”, fully LC-substituted analogues reported previously. Despite the structural irregularity, three out of the four penta-LC-cube derivatives (**II–IV**) show LC transitions, with a tendency to form SmA. LC behavior was characterized using differential scanning calorimetry, polarized light microscopy, and X-ray diffractometry.

## Introduction

Polyhedral silsesquioxanes (POSSs) have received exponentially increasing interest in recent years, mostly as a result of their well-defined structure consisting of a rigid, 0.53 nm inorganic (silica) core which can be directly and covalently bonded to up to eight functional organic groups to provide an organic “surface”.<sup>1–3</sup> One of the major potential applications of POSS materials is as nanosized building blocks for organic/inorganic hybrids with completely defined interfaces and wherein there is exceptional control of the organic architecture between the rigid silica cores.<sup>4,5</sup> While most POSS compounds form amorphous nanocomposites when polymerized or copolymerized,<sup>5</sup> LC-modified derivatives should order in three dimensions and could provide contrasting information about nanocomposite properties. We have recently described the creation of thermoplastic nanocomposites produced using atom-transfer polymerization;<sup>6</sup> here we extend this idea to model thermoplastic LC compounds. Our overall goal is to completely delineate the types of nanocomposite structures available using a structurally defined inorganic core.

In the past few decades, linear polysiloxane and cyclic siloxane based side-chain LC materials have been

studied extensively.<sup>7,8</sup> In principle they can be viewed as 1-D and 2-D analogues of 3-D POSS based LC compounds. LC silsesquioxanes based on  $Q_8M_8^H$  and vinyl-functional mesogens were first reported by Kreuzer et al.<sup>9</sup> Most of these LC cubes exhibit smectic phase behavior. A rodlike (bundle) conformation was suggested because all the compounds are uniaxially positive. Very recently, Mehl et al. synthesized LC cubes with structures similar to those of  $Q_8M_8^H$  and cyanobiphenyl mesogens.<sup>10</sup> With spacer lengths ranging from 4 to 11 carbons, all LC silsesquioxanes exhibited SmA LC behavior.

To the best of our knowledge, all previous POSS based LC compounds involved octasubstituted moieties on a cubic core.<sup>9,10</sup> With an aim of making polymerizable LC cubes and hence nanocomposites, we attempted to leave some reactive vertices for further attachment of polymerizable groups. For this reason, we limited the number of LC side chains attached to the octasilsesquioxane to an average of 4–5, leaving four or three “open” vertices for further functionalization. Compared with octa-LC cubes, such tetra- or penta-LC-substituted cubes are “irregular” in structure, especially taking into account the fact that they should consist of a spectrum of mono-, di-, tri-, tetra-, penta-, hexa-, and even hepta-

<sup>†</sup> University of Michigan.

<sup>‡</sup> Wright-Patterson Air Force Base.

(1) (a) Voronkov, M. G.; Lavrent'yev, V. I. *Top. Curr. Chem.* **1982**, *102*, 199. (b) Baney, R. H.; Itoh, M.; Sakakibara, A.; Suzuki, T. *Chem. Rev.* **1995**, *95*, 1409. (c) Loy, D. A.; Shea, K. J. *Chem. Rev.* **1995**, *95*, 1431. (d) Provatas, A. Matisons, J. G. *Trends Polym. Sci.* **1997**, *5*, 327.

(2) Laine, R. M.; Zhang, C. X.; Sellinger, A.; Viculis, L. *Appl. Organomet. Chem.* **1998**, *12* (10–11), 715.

(3) Schwab, J. J.; Lichtenhan, J. D. *Appl. Organomet. Chem.* **1998**, *12* (10–11), 707.

(4) Hedrick, J. L.; Miller, R. D.; Yoon, D.; Cha, H. J.; Brown, H. R.; Srinivasan, S. A.; Di Pietro, R.; Flores, V.; Hummer, J.; Cook, R.; Liniger, E.; Simonyi, E.; Klaus, D. *Org. Thin Films* **1998**, *695*, 371.

(5) Zhang, C.; Babonneau, F.; Bonhomme, C.; Laine, R. M.; Soles, C. L.; Hristov, H. A.; Yee, A. F. *J. Am. Chem. Soc.* **1998**, *120*, 8380.

(6) Costa, R. O. R.; Tamaki, R.; Vasconcelos, W. L. and Laine, R. M. *Macromolecules* **2001**, *34*, 5398.

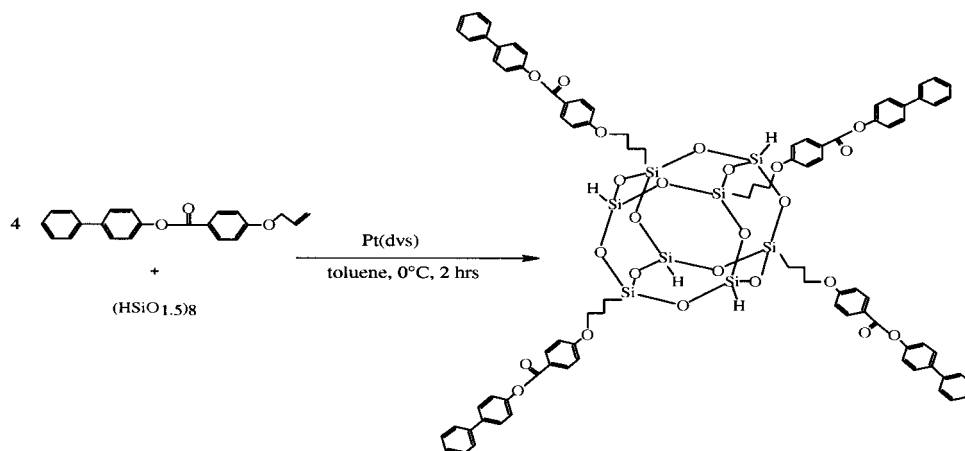
(7) (a) Finkelmann, H. In *Thermotropic Liquid Crystals*; Gray, G. W. Ed.; John Wiley & Sons: 1987, Chapter 6, and references cited therein. (b) *Liquid Crystals*; Baumgartel, H., Franck, E. U., Grunbein, F. W., Eds.; Springer: New York, 1994; pp 116–132.

(8) (a) Kreuzer, F.-H.; Anrejewski, D.; Haas, W.; Haberle, N.; Rieple, G.; Spes, R. *Mol. Cryst. Liq. Cryst. Cryst.* **1991**, *199*, 345. (b) Gresham, K. D.; Mchugh, C. M.; Bunning, T. J.; Crane, R. L.; Klei, H. E.; Samulski, E. T. *J. Polym. Sci., Part A: Polym. Chem.* **1994**, *32*, 2039. (c) Pachter, R.; Bunning, T. J.; Crane, R. L.; Adams, W. W. *Makromol. Chem., Theory Simul.* **1993**, *2*, 337.

(9) Kreuzer, F.-H.; Maurer, R.; Spes, R. *Makromol. Chem. Macromol. Symp.* **1991**, *50*, 215.

(10) (a) Mehl, G. H.; Goodby, J. W. *Angew. Chem., Int. Ed. Engl.* **1996**, *35* (22), 2641. (b) Mehl, G. H.; Thronton, A. J.; Goodby, J. W. *Liq. Cryst.* **1999**, *332*, 455. (c) Saez, I. N.; Goodby, J. W. *Liq. Cryst.* **1999**, *26*, 1101.

## Scheme 1. Tetra-LC-substituted Silsesquioxane



LC cubes. With such additional structural irregularities, together with the restricted topology introduced by the octahedral core, such LC silsesquioxanes should provide excellent models to study the self-organization and ordering patterns of 3-D organic–inorganic entities because they will likely represent materials that are the least likely to order.

In our earlier work, silsesquioxane T<sub>8</sub><sup>H</sup> was reacted with 4-(4-allyloxy-benzoyloxy)biphenyl via Pt catalyzed hydrosilylation to obtain the tetra-LC-substituted (average) silsesquioxane (Scheme 1).<sup>11</sup> This material exhibits nematic behavior at temperatures of 134–178 °C. We describe here efforts to (1) develop partially substituted LC-cube compounds, (2) decrease mesogen melting/LC transition temperatures, and (3) prepare LC cubes with lower transition temperatures through the incorporation of extended spacers, as detailed below. This work is a prelude to studying polymerizable versions of these materials.

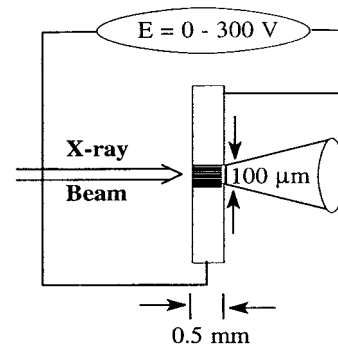
### Experimental Section

**Materials.** Toluene for hydrosilylation was distilled from benzophenone/sodium. Q<sub>8</sub>M<sub>8</sub>H was synthesized following modified literature procedures.<sup>12</sup> Platinum dicyclopentadienyl dichloride complex [Pt(dcp)] was synthesized following literature procedure.<sup>15</sup> Other reagents and solvents were obtained from standard vendors and used as received.

**Techniques.** *NMR Analyses.* All <sup>1</sup>H- and <sup>13</sup>C NMR analyses were done in CDCl<sub>3</sub> and recorded on a Varian INOVA 400 spectrometer. <sup>1</sup>H NMR spectra were collected at 400.0 MHz using a 6000 Hz spectral width, a relaxation delay of 3.5 s, a pulse width of 38°, 30k data points, and CHCl<sub>3</sub> (7.259 ppm) as internal reference. <sup>13</sup>C {<sup>1</sup>H} NMR spectra were obtained at 100.6 MHz using a 25 000 Hz spectral width, a relaxation delay of 1.5 s, a pulse width of 40°, 75k data points, and CDCl<sub>3</sub> (77.23 ppm) as internal reference.

*GC/mass spectral analyses* were conducted on a Finningan model 4021 quadrupole GC/mass spectrometer by electron ionization. Data were recorded and analyzed using the software package provided by Galwin.

*Gel permeation chromatographic analyses* were performed on a Waters GPC system, using a Waters 410 RI detector, Waters Styragel columns (7.8 × 300, HR 0.5, 1, 3, 4), and a PL-DCU data capture unit from Polymer Laboratory. The system was calibrated using polystyrene standards obtained



**Figure 1.** Schematic of X-ray diffraction analysis in an electric field.

from Polymer Laboratory. THF was used as the eluent, at a flow rate of 1.0 mL/min.

*Elemental analysis* samples were submitted to the Department of Chemistry analytical services for analysis of carbon, hydrogen and nitrogen contents. A Perkin-Elmer (Norwalk, CT) 2400 CHN elemental analyzer was operated at 1075 °C, with He as a carrier gas.

*Thermal gravimetric analyses* were performed on a Perkin-Elmer TGA-7 thermogravimetric analyzer (Perkin-Elmer Co., Norwalk, CT). The instrument was calibrated with alumel and iron supplied by Perkin-Elmer. Measurements were performed under a continuous flow of nitrogen or synthetic air (25 mL/min.) at 20 °C/min.

*Differential scanning calorimetry* was performed on a Perkin-Elmer DSC-7 differential scanning calorimeter (Perkin-Elmer Co., Norwalk, CT). The instrument was calibrated with indium supplied by Perkin-Elmer. Measurements were performed under a continuous flow of nitrogen (25 mL/min.). Samples (1–2 mg) were typically equilibrated at 30 °C, ramped to the desired temperature (~20 °C lower than decomposition temperature), and then allowed to cool back to 30 °C at 10 °C/min. Three heating–cooling cycles were recorded for each sample unless otherwise noted.

*Polarized optical microscopic (POM) studies* were conducted using a Nikon Optiphot-Pol microscope, Mettler FP82HT hot stage, and Mettler FP90 Central Processor. A heating rate of 10 °C/min. was used.

*X-ray diffraction studies* of LC compounds were conducted at the Cornell High Energy Synchrotron Source (CHESS) using 0.928 Å radiation. Sample cells consisted of two 0.5 mm gold-plated stainless steel electrodes separated by a controlled gap of 100 μm (see Figure 1). This electrode configuration was held in a Mettler FP 82HT hot stage. Samples were heated above the isotropization temperature within the electrodes and held in place by capillary forces. An AC electric field of 300 V was applied across the electrodes while in the isotropic phase,

(11) Sellinger, A.; Laine, R. M.; Chu, V.; Viney, C. *J. Polym. Sci., Part A: Polym. Chem.* **1994**, *32*, 3069.

(12) (a) Hasegawa, I. *J. Sol–Gel Sci. Technol.* **1993**, *1*, 57. (b) Hasegawa, I.; Motojima, D. *J. Organomet. Chem.* **1992**, *441*, 373.

and the sample was cooled into the temperature region of interest. Nominally, two different frequencies were investigated (10 and 10000 Hz). Incoming X-rays were orthogonal to the direction of the applied electric field. A detailed description of electric field alignment on related siloxane compounds and data acquisition techniques was published by Bunning et al. previously.<sup>13</sup>

*Molecular simulations* were performed using CAChe program (Computer Aided Chemistry, Oxford Molecular Group Inc.). Molecular structures were optimized using Allinger's standard Molecular-Mechanics (MM2) force field.<sup>14</sup> The optimization was generally stopped when the energy change between iterations was within 0.01 cal/mol.

**Synthesis. 1-Allyloxy-3-chloropropane (1).** To a mixture of 5.740 g (0.14 mol) of NaOH and 60 mL of dry THF in a 100 mL round bottom flask equipped with a magnetic stir bar, a reflux condenser, and an addition funnel was added 10 mL (0.12 mol) of 3-chloro-1-propanol. The mixture was stirred at room temperature for 1 h. Then 15.5 mL (0.18 mol) of allyl bromide was added through the dropping funnel. The reaction mixture was refluxed for 15 h. Progress was followed by <sup>1</sup>H NMR and GC/mass spectral analysis. The NaBr produced was removed by washing with 100 mL of water twice in a separatory funnel. The organic layer was dried over anhydrous Na<sub>2</sub>SO<sub>4</sub>. THF was removed using a rotary evaporator. Compound **1** was distilled under vacuum (23–24 °C/(0.05 mmHg)), to yield 12.2 g (80%) of colorless liquid. <sup>1</sup>H NMR (CDCl<sub>3</sub>, ppm): 5.8–6.0 (1H, m), 5.1–5.3 (2H, m), 3.95 (2H, ddd), 3.63 (2H, t), 3.54 (2H, t), 2.00 (2H, p). <sup>13</sup>C NMR (CDCl<sub>3</sub>, ppm): 134.6, 116.8, 71.9, 66.5, 41.9, 32.7. Mass spectral analysis (EI, *m/z*): 134 (P<sup>+</sup>, 0.5%), 107 (P<sup>+</sup> – vinyl, 4.9%), 77 (CH<sub>2</sub>CH<sub>2</sub>CH<sub>2</sub>Cl<sup>+</sup>, 10.1%), 58 (CH<sub>2</sub>=CHCH<sub>2</sub>OH<sup>+</sup>, 81.5%), 41 (CH<sub>2</sub>=CHCH<sub>2</sub><sup>+</sup>, 100%).

**4-[(3-Allyloxy)propanoxy]benzoic acid (2).** To a solution of 20.0 g (0.17 mol) of 4-hydroxybenzoic acid in 150 mL of dimethyl sulfoxide (DMSO) in a 250 mL round bottom flask, was added 24.4 g (0.43 mol) of KOH and traces of KI. The mixture was stirred at room temperature for ~1 h before 23.4 g (0.17 mol) of 1-allyloxy-3-chloropropane (**1**) was added through the addition funnel. The reaction was heated at 120 °C overnight and 150 °C for 4 h. The resulting solution was then chilled in ice, and a dark pink solid was filtered off. This solid was dissolved in 50 mL of H<sub>2</sub>O and titrated with 10% HCl to pH < 3. The white precipitate produced was recrystallized twice from ethanol/H<sub>2</sub>O to yield 19.5 g (58% of theoretical) of white crystals (mp 93 °C). <sup>1</sup>H NMR (CDCl<sub>3</sub>, ppm): 8.05 (2H, d), 6.94 (2H, d), 5.8–6.0 (1H, m), 5.1–5.3 (2H, m), 4.15 (2H, t), 4.00 (2H, ddd), 3.62 (2H, t), 2.10 (2H, p). <sup>13</sup>C NMR (CDCl<sub>3</sub>, ppm): 172.0, 163.5, 134.5, 132.3, 121.6, 117.1, 114.2, 71.9, 66.5, 65.1, 29.5. Mass spectral analysis (EI, *m/z*): 236 (P<sup>+</sup>, 19.3%), 219 (P<sup>+</sup> – OH, 1.3%), 179 (P<sup>+</sup> – CH<sub>2</sub>=CHCH<sub>2</sub>O, 30.6%), 151 (P<sup>+</sup> – CH<sub>2</sub>=CHCH<sub>2</sub>OCH<sub>2</sub>CH<sub>2</sub>, 21.0%), 121 (C<sub>6</sub>H<sub>5</sub>COOH<sup>+</sup>, 29.8%), 99 (CH<sub>2</sub>=CHCH<sub>2</sub>OCH<sub>2</sub>CH<sub>2</sub>CH<sub>2</sub><sup>+</sup>, 33.9%), 57 (CH<sub>2</sub>=CHCH<sub>2</sub>O<sup>+</sup>, 28.8%), 41 (CH<sub>2</sub>=CHCH<sub>2</sub><sup>+</sup>, 100%).

**4-Hydroxy-4'-methoxybiphenyl (3).** The synthesis of **3** followed published procedures with minor modification.<sup>15</sup> To 40 mL of 10% NaOH solution at 0 °C was added 7.5 g (0.040 mol) of 4,4'-dihydroxybiphenyl (biphenol) with vigorous stirring. Dimethyl sulfate was then added slowly to the mixture through an addition funnel. The reaction was stirred at 0 °C for about 1 h. The crude product precipitated from solution and was filtered off. At this point, 0.95 g of the original biphenol was recovered after acidification of the filtrate. The crude product was purified by first dissolving in 10% NaOH solution and then acidifying with 20% HCl. The product, 4-hydroxy-4'-methoxybiphenyl (**3**), was obtained as a colorless crystalline material after recrystallization from ethanol (3.4 g, 75% of theoretical based on amount of biphenol consumed).

<sup>1</sup>H NMR (CDCl<sub>3</sub>, ppm): 7.40 (2H, d), 7.33 (2H, d), 6.88 (2H, d), 6.77 (2H, d), 4.42 (1H, s), 3.71 (3H, s). <sup>13</sup>C NMR (CDCl<sub>3</sub>, ppm): 158.0, 156.3, 132.6, 130.6, 127.1, 126.9, 115.5, 71.9, 114.1, 55.1.

**4-Phenylphenyl 4-[(3-Allyloxy)propanoxy]benzoate (4).** In a 25 mL three-necked flask equipped with a condenser, a magnetic stir bar, and an addition funnel was placed 3.8 g (0.016 mol) of 4-[(3-allyloxy)propanoxy]benzoic acid (**2**). Thionyl chloride, SOCl<sub>2</sub>, 1.8 mL (0.024 mol), was added dropwise through the addition funnel. After the reaction was stirred for 30 min, five drops of dimethylformamide (DMF) were added via syringe. The reaction was stirred at room temperature overnight and then at 60 °C for 1 h. Excess SOCl<sub>2</sub> was removed under vacuum. The yellowish liquid acid chloride thus obtained was used in the following esterification without purification.

In 5 mL of THF, 1.93 g (0.016 mol) of 4-phenylphenol was dissolved in a round bottom flask equipped with a magnetic stirrer, an addition funnel, and a condenser. Et<sub>3</sub>N, 3.0 mL (0.022 mol) in 3 mL of THF, was then added dropwise. The acid chloride obtained above (presumably, 0.016 mol) in 5 mL of THF was added slowly with vigorous stirring at 0 °C. The reaction mixture was allowed to warm slowly and stirred at room temperature for 4 h and refluxed for 1 h. After THF was removed on a rotary evaporator, the brownish solid was dissolved in 30 mL of CH<sub>2</sub>Cl<sub>2</sub>. The CH<sub>2</sub>Cl<sub>2</sub> solution was washed with 40 mL of water, 40 mL of 10% HCl, and dried over anhydrous sodium sulfate. CH<sub>2</sub>Cl<sub>2</sub> was removed via rotary evaporation, and the crude product was recrystallized twice from ethanol/H<sub>2</sub>O. Compound **4** was recovered as white crystals and further purified via silica gel chromatography using hexane/ethyl acetate (5:1) as eluent, giving an 83% yield (mp 103 °C from DSC). Anal. Found (%): C, 77.26; H, 6.50. Calcd: C, 77.30; H, 6.23; O, 16.47. <sup>1</sup>H NMR (CDCl<sub>3</sub>, ppm): 8.20 (2H, d), 7.64 (2H, d), 7.60 (2H, d), 7.45 (2H, t), 7.36 (1H, t), 7.27 (2H, d), 7.02 (2H, d), 5.8–6.0 (1H, m), 5.1–5.3 (2H, m), 4.20 (2H, t), 4.02 (2H, ddd), 3.65 (2H, t), 2.13 (2H, p). <sup>13</sup>C NMR (CDCl<sub>3</sub>, ppm): 164.9, 163.4, 150.4, 140.4, 138.8, 134.7, 132.2, 128.7, 128.1, 127.1, 127.2, 122.0, 121.6, 116.9, 114.2, 71.9, 66.4, 65.1, 29.5. Mass spectral analysis (EI, *m/z*): 388 (P<sup>+</sup>, 5.2%), 219 (P<sup>+</sup> – C<sub>6</sub>H<sub>5</sub>C<sub>6</sub>H<sub>4</sub>O, 100%), 170 (C<sub>6</sub>H<sub>5</sub>C<sub>6</sub>H<sub>4</sub>OH<sup>+</sup>, 50.7%), 99 (CH<sub>2</sub>=CHCH<sub>2</sub>OCH<sub>2</sub>CH<sub>2</sub>CH<sub>2</sub><sup>+</sup>, 29.3%), 57 (CH<sub>2</sub>=CHCH<sub>2</sub>O<sup>+</sup>, 8.9%), 41 (CH<sub>2</sub>=CHCH<sub>2</sub><sup>+</sup>, 50.4%).

**4-(4-Methoxyphenyl)phenyl 4-[(3-Allyloxy)propanoxy]benzoate (5).** 4-(4-Methoxyphenyl)phenyl 4-[(3-allyloxy)propanoxy]benzoate (**5**) was prepared from **2** and **3** following the same procedure as for compound **4**. White crystals of **5** were obtained after recrystallization in ethanol/H<sub>2</sub>O and purification via silica gel chromatography using hexane/ethyl acetate (5:1) as eluent, with a 90% yield. Compound **5** exhibits nematic texture between 111 and 208 °C (polarized light microscopy). Anal. Found (%): C, 74.67; H, 6.50. Calcd: C, 74.62; H, 6.26; O, 19.12. <sup>1</sup>H NMR (CDCl<sub>3</sub>, ppm): 8.17 (2H, d), 7.59 (2H, d), 7.53 (2H, d), 7.25 (2H, d), 7.00 (2H, t), 6.99 (2H, d), 5.8–6.0 (1H, m), 5.1–5.3 (2H, m), 4.18 (2H, t), 4.01 (2H, ddd), 3.86 (3H, s), 3.64 (2H, t), 2.120 (2H, p). <sup>13</sup>C NMR (CDCl<sub>3</sub>, ppm): 165.2, 163.6, 159.4, 150.2, 138.7, 135.0, 133.2, 132.5, 128.3, 127.9, 122.2, 121.9, 117.1, 114.5, 114.4, 72.2, 65.7, 65.4, 55.5, 29.8. Mass spectral analysis (EI, *m/z*): 418 (P<sup>+</sup>, 17.2%), 277 (P<sup>+</sup> – CH<sub>2</sub>=CHCH<sub>2</sub>, 1.6%), 219 (P<sup>+</sup> – CH<sub>3</sub>OC<sub>6</sub>H<sub>4</sub>C<sub>6</sub>H<sub>4</sub>O, 100%), 199 (CH<sub>3</sub>OC<sub>6</sub>H<sub>5</sub>C<sub>6</sub>H<sub>4</sub>OH<sup>+</sup>, 13.0%), 99 (CH<sub>2</sub>=CHCH<sub>2</sub>OCH<sub>2</sub>CH<sub>2</sub>CH<sub>2</sub><sup>+</sup>, 17.5%), 57 (CH<sub>2</sub>=CHCH<sub>2</sub>O<sup>+</sup>, 4.9%), 41 (CH<sub>2</sub>=CHCH<sub>2</sub><sup>+</sup>, 23.6%).

**Allyl 2-(2-Chloroethoxy)ethyl Ether (6).** Following the procedure used for 1-allyloxy-3-chloro-propane (**1**), compound **6** was prepared from 20 mL (0.19 mol) of 2-(2-chloroethoxy)-ethanol, 21.3 mL (0.25 mol) of allyl bromide, and 9.105 g (0.23 mol) of NaOH. The product **6** was distilled under vacuum (38–41 °C/(0.05 mmHg)), to provide 24.8 g of colorless liquid (82% of theory). <sup>1</sup>H NMR (CDCl<sub>3</sub>, ppm): 5.8–6.0 (1H, m), 5.1–5.3 (2H, m), 3.99 (2H, ddd), 3.5–3.8 (8H, m). <sup>13</sup>C NMR (CDCl<sub>3</sub>, ppm): 134.5, 117.0, 72.1, 71.2, 70.5, 69.2, 42.5. Mass spectral analysis (EI, *m/z*): 164 (P<sup>+</sup>, 0.5%), 107 (CH<sub>2</sub>CH<sub>2</sub>OCH<sub>2</sub>CH<sub>2</sub>Cl<sup>+</sup>, 16.5%), 93 (CH<sub>2</sub>OCH<sub>2</sub>CH<sub>2</sub>Cl<sup>+</sup>, 13.0%), 71 (CH<sub>2</sub>=CHOCH<sub>2</sub><sup>+</sup>, 20.7%), 63 (CH<sub>2</sub>CH<sub>2</sub>Cl<sup>+</sup>, 81.4%), 41 (CH<sub>2</sub>=CHCH<sub>2</sub><sup>+</sup>, 100%).

(13) Bunning, T. J.; Korner, H.; Tsukruk, V. V.; McHugh, C. M.; Ober, C. K.; Adams, W. W. *Macromolecules* **1996**, *29*, 8717.

(14) Allinger, N. L. *J. Am. Chem. Soc.* **1977**, *99*, 8127.

(15) Apfel, M. A.; Finkelmann, H.; Janini, G. M.; Laub, R. J.; Luhmann, B.-H.; Price, A.; Roberts, W. L.; Shaw, T. J.; Smith, C. A. *Anal. Chem.* **1985**, *57*, 651.



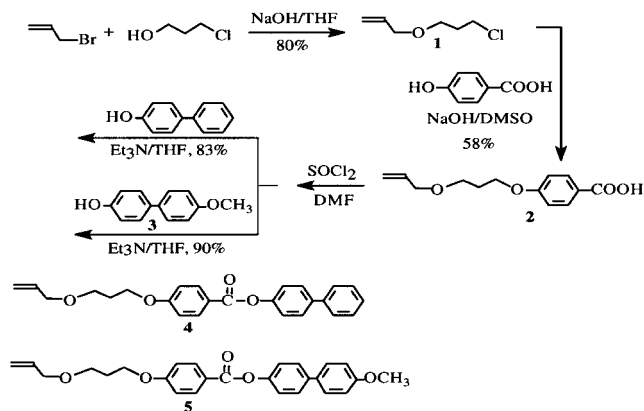
4-[2-(2-Allyloxyethoxy)ethoxy]benzoic acid (**7**). The synthetic procedure for 4-[2-(2-allyloxyethoxy)ethoxy]benzoic acid (**7**) was the same as for compound **2**. Compound **7** was recovered in 56% yield after recrystallization from ethanol/H<sub>2</sub>O (mp 89 °C). <sup>1</sup>H NMR (CDCl<sub>3</sub>, ppm): 8.04 (2H, d), 6.95 (2H, d), 5.8–6.0 (1H, m), 5.1–5.3 (2H, m), 4.20 (2H, t), 4.04 (2H, ddd), 3.89 (2H, t), 3.75 (2H, t), 3.64 (2H, t). <sup>13</sup>C NMR (CDCl<sub>3</sub>, ppm): 171.7, 163.2, 134.5, 132.3, 121.8, 117.3, 114.2, 72.3, 70.9, 69.5, 69.4, 67.6. Mass spectral analysis (EI, *m/z*): 266 (P<sup>+</sup>, 8.9%), 209 (P<sup>+</sup> – CH<sub>2</sub>=CHCH<sub>2</sub>O, 14.1%), 165 (P<sup>+</sup> – CH<sub>2</sub>=CHCH<sub>2</sub>OCH<sub>2</sub>CH<sub>2</sub>O, 51.3%), 138 (OC<sub>6</sub>H<sub>4</sub>COOH<sup>+</sup>, 60.9%), 121 (C<sub>6</sub>H<sub>5</sub>COOH<sup>+</sup>, 94.1%), 41 (CH<sub>2</sub>=CHCH<sub>2</sub><sup>+</sup>, 100%).

4-Phenylphenyl 4-[2-(2-allyloxyethoxy)ethoxy]benzoate (**8**). Monomer **8** was synthesized following the same procedure as for monomer **4** from **7** and 4-phenylphenol. White crystals of **8** were obtained after recrystallization in ethanol/H<sub>2</sub>O and purification by silica gel column chromatography using hexane/ethyl acetate (5:1) as eluent, with a yield of 83% of theory (mp 63 °C from DSC). Anal. Found (%): C, 74.06; H, 6.58. Calcd: C, 74.62; H, 6.26; O, 19.12. <sup>1</sup>H NMR (CDCl<sub>3</sub>, ppm): 8.17 (2H, d), 7.64 (2H, d), 7.60 (2H, d), 7.45 (2H, t), 7.36 (1H, t), 7.28 (2H, d), 7.02 (2H, d), 5.8–6.0 (1H, m), 5.1–5.3 (2H, m), 4.24 (2H, t), 4.05 (2H, ddd), 3.92 (2H, t), 3.77 (2H, t), 3.65 (2H, t). <sup>13</sup>C NMR (CDCl<sub>3</sub>, ppm): 164.9, 163.2, 150.5, 140.5, 138.9, 134.2, 132.3, 128.8, 128.2, 127.3, 127.3, 122.6, 122.1, 117.3, 114.4, 72.3, 71.0, 69.6, 69.5, 67.7. Mass spectral analysis (EI, *m/z*): 418 (P<sup>+</sup>, 2.1%), 249 (P<sup>+</sup> – C<sub>6</sub>H<sub>5</sub>C<sub>6</sub>H<sub>4</sub>O, 100%), 170 (C<sub>6</sub>H<sub>5</sub>C<sub>6</sub>H<sub>4</sub>OH<sup>+</sup>, 14.4%), 129 (CH<sub>2</sub>=CHCH<sub>2</sub>O – CH<sub>2</sub>CH<sub>2</sub>OCH<sub>2</sub> – CH<sub>2</sub><sup>+</sup>, 17.7%), 85 (CH<sub>2</sub>=CHCH<sub>2</sub>OCH<sub>2</sub>CH<sub>2</sub><sup>+</sup>, 12.1%), 41 (CH<sub>2</sub>=CHCH<sub>2</sub><sup>+</sup>, 30.9%).

4-(4-Methoxyphenyl)phenyl 4-[2-(2-allyloxyethoxy)ethoxy]benzoate (**9**). Monomer **9** was synthesized, following the same procedure as that for monomer **4**, from **7** and **3**. White crystals of **9** were obtained after recrystallization from ethanol/H<sub>2</sub>O followed by purification via silica gel column chromatography using hexane/ethyl acetate (5:1) as the eluent, with a yield of 87% of theoretical (mp 121 °C from DSC). Anal. Found (%): C, 72.16; H, 6.56. Calcd: C, 72.30; H, 6.29; O, 21.41. <sup>1</sup>H NMR (CDCl<sub>3</sub>, ppm): 8.16 (2H, d), 7.58 (2H, d), 7.52 (2H, d), 7.25 (2H, d), 7.01 (1H, d), 7.00 (2H, d), 5.8–6.0 (1H, m), 5.1–5.3 (2H, m), 4.24 (2H, t), 4.05 (2H, ddd), 3.91 (2H, t), 3.85 (3H, s), 3.75 (2H, t), 3.65 (2H, t). <sup>13</sup>C NMR (CDCl<sub>3</sub>, ppm): 165.0, 163.1, 160.9, 150.2, 138.7, 134.9, 133.2, 132.4, 128.4, 127.9, 122.2, 117.4, 114.6, 114.4, 72.5, 71.1, 69.8, 69.6, 67.9. Mass spectral analysis (EI, *m/z*): 448 (P<sup>+</sup>, 31.0%), 249 (P<sup>+</sup> – CH<sub>3</sub>OC<sub>6</sub>H<sub>4</sub>C<sub>6</sub>H<sub>4</sub>O, 100%), 227 (CH<sub>3</sub>OC<sub>6</sub>H<sub>4</sub>C<sub>6</sub>H<sub>4</sub>OC=O<sup>+</sup>, 6.6%), 199 (CH<sub>3</sub>OC<sub>6</sub>H<sub>4</sub>C<sub>6</sub>H<sub>4</sub>O<sup>+</sup>, 11.1%), 41 (CH<sub>2</sub>=CHCH<sub>2</sub><sup>+</sup>, 13.5%).

LC-Cube **I** from Monomer **4**. LC-cube **I** was synthesized from Q<sub>8</sub>M<sub>8</sub><sup>H</sup> and LC monomer **4**. Cube Q<sub>8</sub>M<sub>8</sub><sup>H</sup> (0.150 g, 0.147 mmol) and monomer **4** (0.277 g, 0.662 mmol) were placed in a 50 mL Schlenk flask. The flask was degassed and refilled with N<sub>2</sub> three times. Distilled toluene (13 mL) was added to dissolve the solids, followed by 5 drops of 2.0 mM Pt(dcp) solution. After the reaction was stirred at room temperature overnight, <sup>1</sup>H NMR analysis indicated an average of ~3.5 LC monomers attached. The reaction was heated at 100 °C overnight, increasing the number of LCs to approximately four per cube. Toluene was removed under N<sub>2</sub> stream, and the crude product was subjected to GPC analysis, which showed excess LC monomer ~ 458 Da. The product was dissolved in toluene and precipitated into hexane three times to remove the LC monomers, as followed by GPC analysis. The resultant product was further recrystallized from CH<sub>2</sub>Cl<sub>2</sub>/hexanes to provide a white powder in 66% yield. NMR and elemental analyses of the final product indicated that about five LC mesogens were attached to each cube on average. Anal. Found (%): C, 57.31; H, 6.05. Calcd (for penta-LC cube): C, 57.21; H, 5.99; O, 21.62; Si, 15.18. <sup>1</sup>H NMR (CDCl<sub>3</sub>, ppm): 8.16 (9.8 H, d), 7.62 (10.1 H, d), 7.59 (10.1 H, d), 7.44 (10.4 H, t), 7.35 (5.2 H, t), 7.27 (10.0 H, d), 6.99 (10.0 H, d), 4.75 (2.2 H, m, Si-H unreacted), 4.16 (10.0 H, t), 3.61 (10.1 H, t), 3.42 (10.1 H, t), 2.09 (10.0 H, p), 1.65 (10.1 H, p), 0.62 (9.5 H, t), 0.26 [14.4 H, d, Si(CH<sub>3</sub>)<sub>2</sub>H], 0.17 [28.8 H, s, Si(CH<sub>3</sub>)<sub>2</sub>C-]. <sup>13</sup>C NMR (CDCl<sub>3</sub>, ppm): 164.9, 163.4, 150.5, 140.4, 138.8, 132.3, 128.8, 128.2, 127.3, 127.1, 122.1, 121.6, 114.3, 73.7, 67.0, 65.3, 29.6, 23.2, 13.7, 0.2 [Si-

## Scheme 2. Synthetic Sequences for **4** and **5**




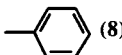
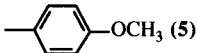
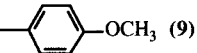
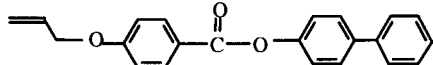
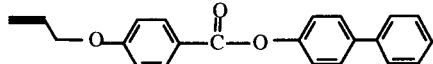
(CH<sub>3</sub>)<sub>2</sub>H], –0.4 [Si(CH<sub>3</sub>)<sub>2</sub>C-]. GPC indicated a narrow distribution: *M<sub>n</sub>* 3.18 × 10<sup>3</sup>, *M<sub>w</sub>* 3.31 × 10<sup>3</sup>, PDI 1.04 (calc. *M<sub>w</sub>* for penta-LC cube: 2960). TGA (ceramic yield in air): 32.9% (theoretical 32.4%).

LC-Cube **II** from Monomer **5**. LC-cube **II** was synthesized from Q<sub>8</sub>M<sub>8</sub><sup>H</sup> and LC compound **5** following the same procedure as used for reaction of Q<sub>8</sub>M<sub>8</sub><sup>H</sup> and monomer **4** as shown above. The product was also purified by dissolving in toluene and reprecipitating in hexane to remove the excess monomer. A final recrystallization gave **II** as a white powder in 60% yield. NMR and elemental analyses of the final product indicated that about five LC mesogens were attached to each cube on average. Anal. Found (%): C, 56.28; H, 6.10. Calcd (for penta-LC cube): C, 56.38; H, 6.03; O, 23.15; Si, 14.45. <sup>1</sup>H NMR (CDCl<sub>3</sub>, ppm): 8.15 (10.0 H, d), 7.57 (10.5 H, d), 7.51 (10.0 H, d), 7.23 (10.3 H, t), 7.00 (20.5 H, d), 4.75 (2.3 H, m, Si-H unreacted), 4.15 (10.2 H, t), 3.85 (14.9 H, s), 3.60 (10.2 H, t), 3.41 (10.2 H, t), 2.09 (10.4 H, p), 1.65 (10.0 H, p), 0.62 (9.8 H, t), 0.26 [14.7 H, d, Si(CH<sub>3</sub>)<sub>2</sub>H], 0.16 [29.8 H, s, Si(CH<sub>3</sub>)<sub>2</sub>C-]. <sup>13</sup>C NMR (CDCl<sub>3</sub>, ppm): 165.2, 163.6, 159.4, 150.2, 138.7, 133.2, 132.5, 128.3, 127.9, 122.2, 122.7, 114.3, 73.7, 67.0, 65.3, 55.3, 29.6, 23.2, 13.7, 0.2 [Si(CH<sub>3</sub>)<sub>2</sub>H], –0.4 [Si(CH<sub>3</sub>)<sub>2</sub>C-]. GPC indicated a narrow distribution: *M<sub>n</sub>* 3.62 × 10<sup>3</sup>, *M<sub>w</sub>* 3.75 × 10<sup>3</sup>, PDI 1.04 (calc. *M<sub>w</sub>* for penta-LC cube: 3110). TGA (ceramic yield in air): 32.6% (theoretical 30.9%).

LC-Cube **III** from Monomer **8**. LC-cube **III** was synthesized from Q<sub>8</sub>M<sub>8</sub><sup>H</sup> and LC compound **8** following the same procedure as used for the reaction of Q<sub>8</sub>M<sub>8</sub><sup>H</sup> and monomer **8**. The product was also purified by dissolving in toluene and reprecipitating in hexane. Final recrystallization gave a white powder of **III** in 54% yield. NMR and elemental analyses of the final product indicated that about five LC mesogens were attached to each cube on average. Anal. Found (%): C, 56.34; H, 6.13. Calcd (for penta-LC cube): C, 56.38; H, 6.03; O, 23.15; Si, 14.45. <sup>1</sup>H NMR (CDCl<sub>3</sub>, ppm): 8.17 (10.2 H, d), 7.63 (9.7 H, d), 7.59 (9.7 H, d), 7.45 (9.3 H, t), 7.35 (4.7 H, t), 7.27 (10.0 H, d), 7.01 (9.2 H, d), 4.75 (3.0 H, m, Si-H unreacted), 4.22 (9.1 H, t), 3.91 (9.4 H, ddd), 3.74 (9.4 H, t), 3.64 (9.2 H, t), 3.46 (9.2 H, t), 1.65 (10.3 H, p), 0.62 (9.3 H, t), 0.26 [17.2 H, d, Si(CH<sub>3</sub>)<sub>2</sub>H], 0.16 [30.1 H, s, Si(CH<sub>3</sub>)<sub>2</sub>C-]. <sup>13</sup>C NMR (CDCl<sub>3</sub>, ppm): 165.1, 163.3, 150.6, 140.6, 138.9, 132.3, 129.0, 128.2, 127.3, 127.3, 122.2, 122.1, 114.4, 74.2, 71.1, 70.2, 69.7, 67.9, 23.3, 13.8, 0.3 [Si(CH<sub>3</sub>)<sub>2</sub>H], –0.2 [Si(CH<sub>3</sub>)<sub>2</sub>C-]. GPC indicated a narrow distribution: *M<sub>n</sub>* 3.55 × 10<sup>3</sup>, *M<sub>w</sub>* 3.69 × 10<sup>3</sup>, PDI 1.04 (calc. *M<sub>w</sub>* for penta-LC cube: 3110). TGA (ceramic yield in air): 29.8% (theoretical 30.9%).

LC-Cube **IV** from Monomer **9**. LC-cube **IV** was synthesized from Q<sub>8</sub>M<sub>8</sub><sup>H</sup> and LC compound **9** following the same procedure as that for the reaction of Q<sub>8</sub>M<sub>8</sub><sup>H</sup> and monomer **9**. The product was purified by dissolving in toluene and precipitating with hexane. Final recrystallization gives **IV** as a white powder in 58% yield. NMR and elemental analyses of the final product indicate that about five LC mesogens were attached to each cube on average. Anal. Found (%): C, 54.54; H, 6.05. Calcd (for penta-LC cube): C, 55.62; H, 6.06; O, 24.53; Si, 13.78. Calcd (for tetra-LC cube): C, 52.96; H, 6.02; O, 25.03; Si, 15.98.

Table 1. Melting Points and LC Transition Temperatures of Mesogens 4, 5, 8, and 9

R	thermal transitions	R	thermal transitions
 (4)	k 103 i	 (8)	k 63 i
 (5)	k 67 n 205 i	 (9)	k 121 i
Compared with:			
			k 141 n 143 i
			k 132 i

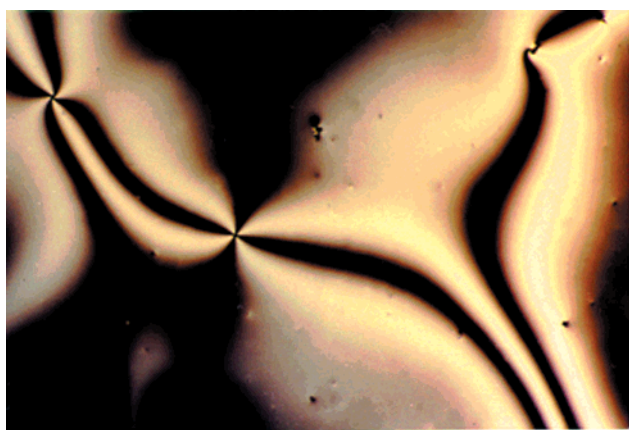
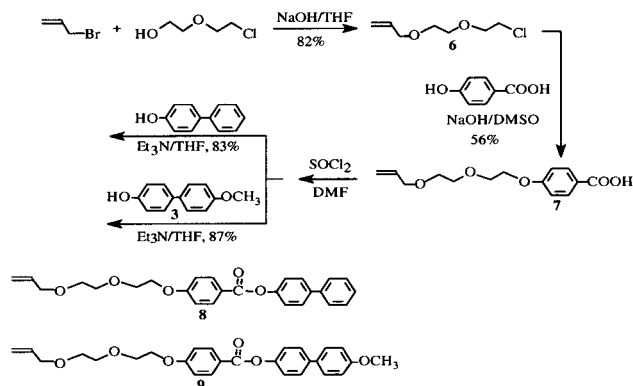


Figure 2. Polarized optical micrograph of the Schlieren texture exhibited by 5 at 180 °C, on cooling from isotropic phase.

Scheme 3. Synthetic Sequences for 8 and 9



<sup>1</sup>H NMR (CDCl<sub>3</sub>, ppm): 8.15 (10.0 H, d), 7.57 (10.7 H, d), 7.51 (10.8 H, d), 7.25 (11.0 H, d), 6.99 (10.8 H, d), 6.97 (10.7 H, d), 4.75 (2.9 H, m, Si-H unreacted), 4.21 (10.5 H, t), 3.89 (11.7 H, t), 3.85 (16.0 H, s), 3.73 (10.5 H, t), 3.62 (10.4 H, t), 3.45 (10.6 H, t), 1.65 (9.4 H, p), 0.60 (9.3 H, t), 0.26 [18.6 H, d, Si-(CH<sub>3</sub>)<sub>2</sub>H], 0.16 [33.9 H, s, Si-(CH<sub>3</sub>)<sub>2</sub>C-]. <sup>13</sup>C NMR (CDCl<sub>3</sub>, ppm): 165.0, 163.3, 160.1, 150.2, 138.7, 133.2, 132.4, 128.3, 127.9, 122.2, 114.6, 114.4, 74.2, 71.2, 70.2, 69.7, 67.9, 55.6, 23.3, 13.8, 0.4 [Si(CH<sub>3</sub>)<sub>2</sub>H], -0.2 [Si(CH<sub>3</sub>)<sub>2</sub>C-]. GPC indicated a narrow distribution: *M*<sub>n</sub> 3.66 × 10<sup>3</sup>, *M*<sub>w</sub> 3.87 × 10<sup>3</sup>, PDI 1.06 (calcd *M*<sub>w</sub> for penta-LC cube: 3260). TGA (ceramic yield in air): 35.0% (theoretical 34.1%).

## Results and Discussion

This work is discussed in three sections: (1) synthesis and characterization of LC mesogenic monomers, (2) synthesis and characterization of LC cubes, and (3) LC behavior of LC cubes.

**Synthesis and Characterization of LC Mesogens.** Rigid-rod mesogens with extended spacers were synthesized and used to prepare LC silsesquioxanes of potential use in preparing nanocomposites, especially for use as dental restoratives.<sup>16</sup> Dual goals were to create materials with LC transitions at biologically important temperatures such that following LC ordering, it would be possible to induce polymerization while retaining ordering.

Two groups of mesogens were synthesized on the basis of two different spacers. Polymethylene chains with terminal olefins are often used as spacers for SCLCP and oligomeric LC materials.<sup>17</sup> The introduction of ether links to polymethylene spacers provides additional flexibility that may further reduce melting points. Thus, our efforts were directed toward preparing flexible ether spacers from allyl bromide and 3-chloro-1-propanol or 2-ethoxyethanol.<sup>18</sup> The synthesis and characterization of the prospective LC mesogens are discussed below.

The first set of compounds was prepared following the sequences shown in Scheme 2. The reaction of allyl bromide with 3-chloro-1-propanol provides the flexible 1-allyloxy-3-chloropropane spacer (1) in good yield. The S<sub>N</sub>2 substitution reaction of 1 and 4-hydroxybenzoic acid required heating in DMSO, ~60% yield of 4-(3-allyloxy)propanoxybenzoic acid (2). Transformation of 2 to its acid chloride and then to compounds 4 and 5 was carried out using standard procedures. Compounds 4 and 5 were obtained as white crystalline compounds following purification.

Table 1 lists the melting points and LC transition temperatures for 4 and 5 as determined by DSC and confirmed by polarized light microscopy (POM). Under

(16) Zhang, C. Ph.D. dissertation, University of Michigan, 1999.

(17) (a) Finkelmann, H.; Ringsdorf, H.; Wendorff, H. *Makromol. Chem.* **1978**, 179, 273; (b) Finkelmann, H.; Happ, M.; Portugal, M.; Ringsdorf, H. *Makromol. Chem.* **1978**, 179, 2541.

(18) Zhang, C.; Laine, R. M. *Polym. Prepr., Div. Polym. Chem., ACS* **1997**, 38, 120.

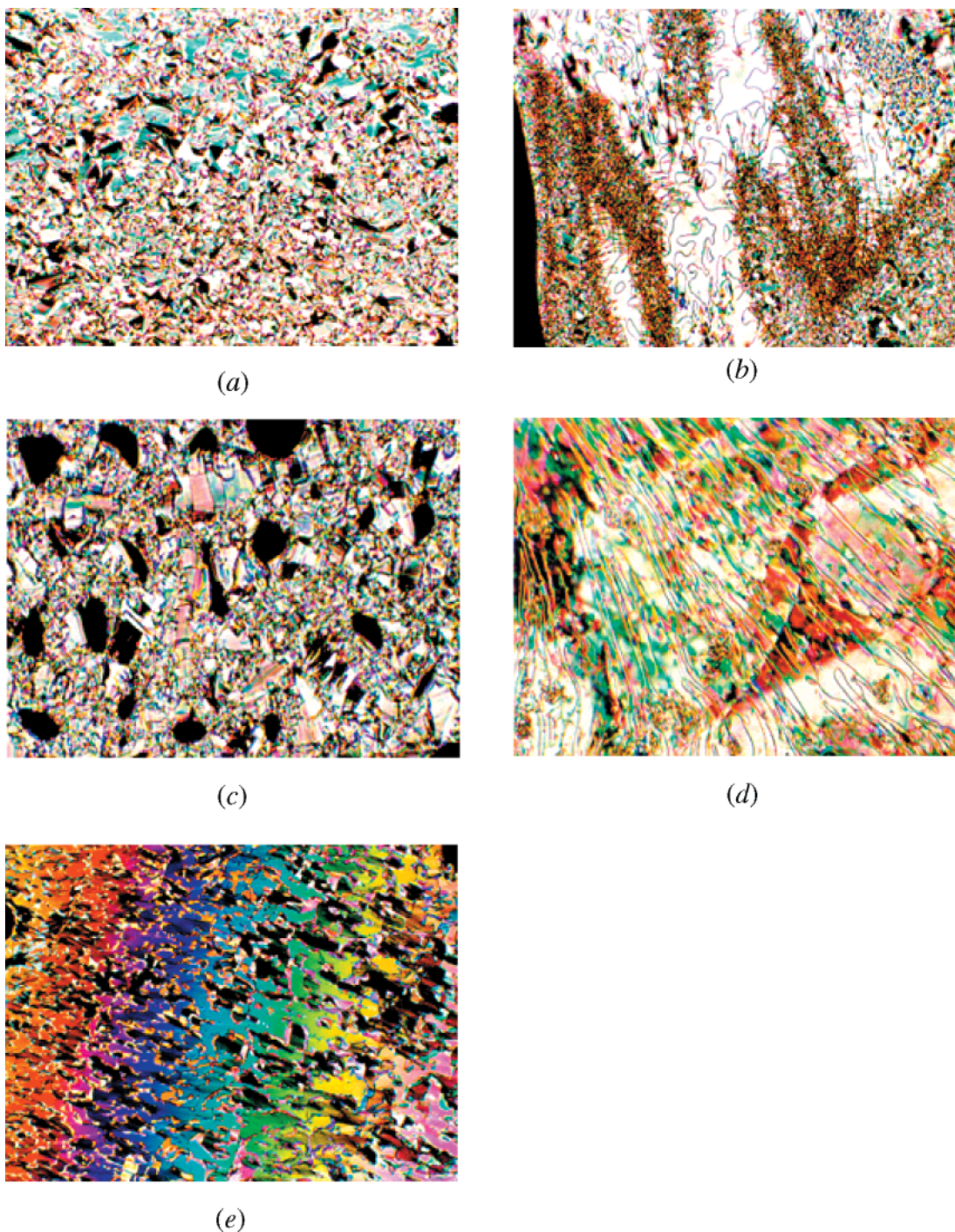




Table 2. LC behavior of LC-cubes I–IV

cubes	substituents	n <sup>a</sup>	dec. temp in N <sub>2</sub> (°C)	SiO <sub>2</sub> ceramic yield in air (theor, %)	LC transitions <sup>b</sup> (°C)
I	4	5	250	32.9 (32.5)	k 138 i 127 k
II	5	5	280	32.6 (30.9)	k 148 Sa 177 n 189 i 181 n 174 Sa 110 k
III	8	5	230	29.8 (30.9)	k 90 Sa 113 i 103 Sa 72 k
IV	9	4	270	35.0 (34.2)	k 123 Sa 156 n 158 i 157 n 154 Sa 83 k

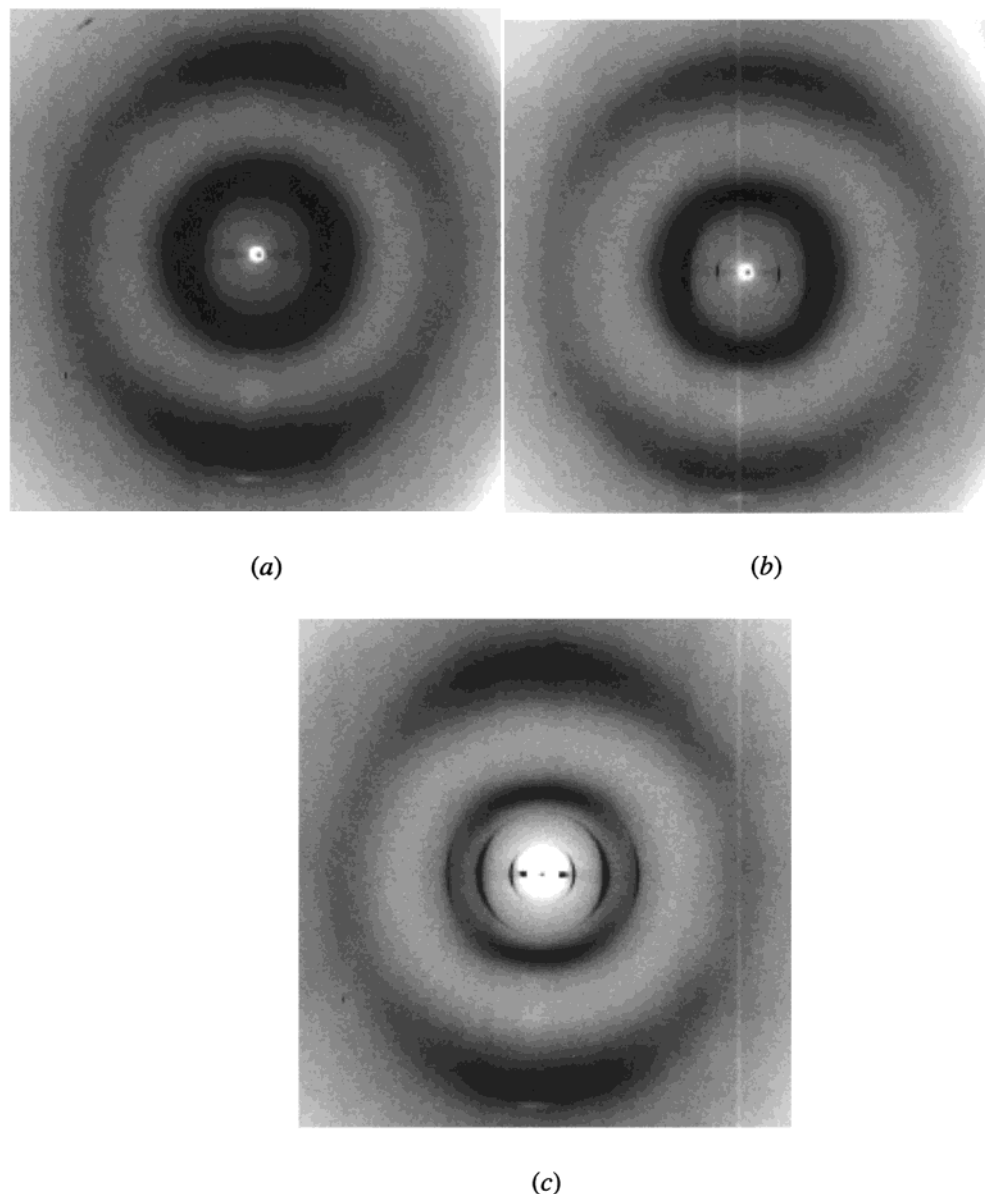
<sup>a</sup> Average number of LC substituents per cube. <sup>b</sup>From second heating/cooling cycles of DSC analysis.



**Figure 4.** POM micrographs of LC-cubes II–IV: (a) II-S<sub>m</sub>A at 155 °C; (b) II-S<sub>m</sub>A/N at 180 °C; (c) III-S<sub>m</sub>A at 100 °C; (d) IV-N at 155 °C; (e) IV-S<sub>m</sub>A at 130 °C.

are stable to  $\approx 280$  °C/N<sub>2</sub>, typical of organic compounds. Ceramic yields are close to theoretical calculations for the average degree of substitution.

**LC Behavior of I–IV.** Thermal transitions for cubes I–IV were first studied by DSC, and then the phase textures were examined using POM. Finally, X-ray



**Figure 5.** X-ray diffraction patterns of LC-cube **II**-nematic (a) and -smectic A (b) and LC-cube **III**-smectic A (c).

diffraction studies were used to confirm the tentative assignments made on the basis of POM.

Compound **I** does not exhibit any LC behavior by DSC, while **II–IV** do. The transition temperatures are listed in Table 2. The phase transitions are generally broad as expected because of the distribution of differently substituted cubes.

A comparison of the phase transitions of **4**, **5**, **8**, and **9** with those of **I–IV** indicates that while nonmesomorphic **4** forms nonmesomorphic cube **I**, nematic mesogen **5** forms **II** which exhibits both SmA and N phases, and nonmesomorphic compounds **8** and **9** give **III** and **IV** which show both SmA and N phases. It appears that covalently attaching rigid and nonmesomorphic groups to silsesquioxane cores enables them to form LC phases, even when the cores are irregularly substituted.

Similar trends were also observed with SCLCPs.<sup>7</sup> In SCLCPs, this behavior was attributed to increased density of mesogens—those attached to polymer backbones are more densely packed and hence organize more easily into LC phases.<sup>7</sup> This may be one reason that

rigid organic units attached to cubes, even irregularly, tend to also form LC phases. An additional observation is that these new materials tend to form “bundle” conformations in their LC phases (see below), wherein the (average) five mesogens per cube are preassembled covalently, decreasing the entropy of the whole system greatly, compared to systems with individual mesogens. This then represents an alternate/additional explanation for why LC phase formation is favored for **II–IV**.

The Table 2 transition temperatures also indicate that **III** and **IV**, with more flexible ethyleneoxy spacers, have lower melting and clearing temperatures than **I** and **II**, respectively, which have stiffer propaneoxy spacers. Introduction of polar methoxy groups (i.e. **5** and **9**) increase the thermal transition temperatures of the corresponding LC cubes (**II** and **IV**, respectively). These observations are consistent with what is known about SCLCPs.<sup>20</sup> There is still room to reduce the transition

(20) Percec, V.; Pugn, C. In *Side Chain Liquid Crystal Polymers*; McArdle, C. B., Ed.; Blackie: Glasgow, 1989; Chapter 3.



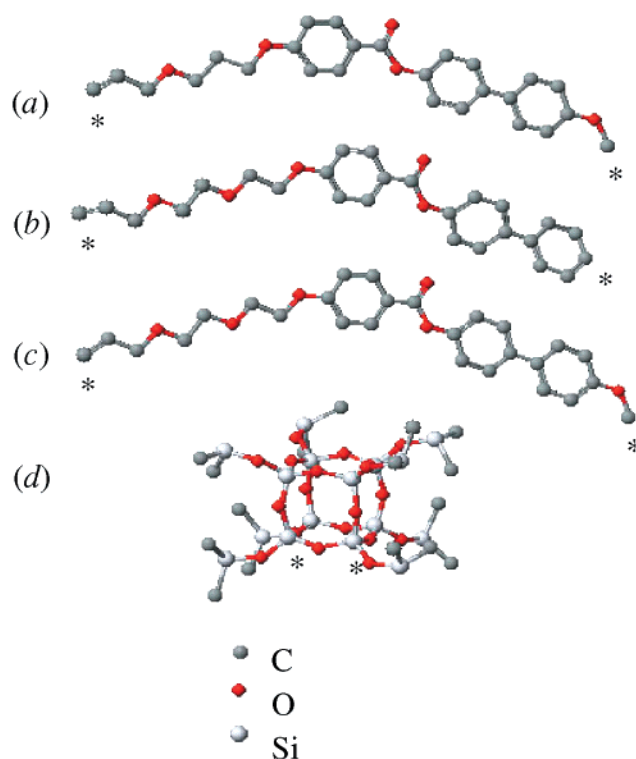
temperatures through the judicious introduction of flexible polymerizable components at the Si–H positions that remain after attachment of **4**, **5**, **8**, and **9**. This could work as long as LC phase formation is not simultaneously inhibited.

The phase textures of **II–IV** were examined using POM. Cube **II** exhibits both the broken focal–conic fan texture of a smectic phase and a threaded marble texture typical of nematic phases.<sup>21</sup> Cube **III** shows smectic phase texture similar to that of **II**. Cube **IV** exhibits both smectic (truncated focal–conic fan type) and nematic (threaded marble type) phases similar to **II**. Figure 4 provides polarized optical micrographs of **II–IV**. The LC cubes exhibit low viscosities in their LC phases, as anticipated.

X-ray studies of **II–IV** indicated diffraction patterns typical of aligned nematic and smectic A phases. Parts a and b of Figure 5 show the diffraction patterns of **II** on cooling in an applied 10 Hz field. The field direction is vertical. There is strong, liquidlike diffuse scattering at a  $d$  spacing of 11–12 Å indicative of Si–O clusters as seen previously.<sup>9,10</sup> This type of scattering is observed in some siloxane-based LCPs and in some siloxane core-based LC macromolecules.<sup>22,23</sup> In addition to being present in the nematic and smectic phases, this strong scattering was also present in the isotropic phase of these compounds. When cooled into the nematic phase, an aligned wide-angle diffraction peak at 4–6 Å is observed. The anisotropy in the diffraction ring indicates the mesogenic units have been aligned by the electric field. Surprisingly, the alignment suggests that the mesogens are perpendicular to the applied field, which suggests negative dielectric anisotropy. All three compounds are similar in their behavior. Surface alignment is ruled out as no alignment occurs on cooling with the field off. Little diffraction is observed in the small-angle region while in the nematic phase. Given the large bulky nature of the molecule, considerable alignment is achieved. This is attributed to the highly flexible spacer units being coupled with the flexible Si–O entities.

Upon cooling into the smectic phase, two sharp aligned small-angle reflections are observed for cube **II** at spacings corresponding to 28–30 and 14–15 Å. The  $d$  spacings for all three cubes were similar. These reflections correspond to the first- and second-order smectic-A peaks. The second order is considerably stronger in intensity than the first order. These peaks are sharp, and estimation of the correlation lengths using the Scherrer equation gives 50 nm. Compounds **III** and **IV** both exhibit a third-order peak as well, as indicated in Figure 5

No splitting (typical of a SmC phase) of the wide- or small-angle peaks is observed. All three compounds exhibit alignment of the mesogens perpendicular to the electric field direction. One interesting observation is a redistribution of the diffuse liquidlike scattered intensity at 11–12 Å in the smectic phase upon alignment, as shown in Figure 5c. Similar to the wide-angle reflection, more intensity on the meridian is observed.



**Figure 6.** CACHE simulation of LC mesogens **5** (a), **8** (b), **9** (c), and cube  $Q_8H_8^H$  (d). [Note: (1) H atoms are not shown; (2) atom(\*) to atom(\*) distances are 24.7 (a), 25.4 (b), 26.5 (c), and 3.1 Å (d).]

This indicates that the cage distribution is also affected upon alignment.

Molecular modeling studies were performed to calculate lengths of the vinyl functionalized LC mesogens, **5**, **8**, and **9**, and the size of the cube using the CACHE program. Molecular conformations were optimized using Allinger's standard molecular-mechanics force field.<sup>14</sup> The results are shown in Figure 6, with mesogen lengths for **5**, **8**, and **9** at 24.7, 25.4, and 26.5 Å, respectively. The Si–Si lateral distance in the  $Q_8M_8^H$  cube is 3.1 Å. The first-order  $d$  spacing of **II–IV** obtained above are approximately equal to the mesogen length plus the cube width (Figure 6), which suggests overlapping of the aromatic units between neighboring layers.

## Conclusions

In this work, organic–inorganic hybrid compounds **I–IV** were synthesized from  $Q_8M_8^H$  and rigid organic units containing extended flexible spacers using Pt(dcp) catalyzed hydrosilylation. Compounds **I–IV** have five side chains on average, different from octa-LC cubes reported previously. However, **II–IV** organize into SmA phases, similar to the octa analogues. A comparison of  $d$  spacings of the SmA phases determined by X-ray diffraction studies with the lengths of LC mesogens and size of the cubic core indicate overlapping of the LC mesogens in the SmA layers. Further study is needed for a complete understanding of the molecular packing mode, the influence of the number of side chains, length and structure of spacers groups, and mesogens on the macroscopic properties of the LC cubes. These results provide the basis for future work on producing LC cubes

(21) *Smectic Liquid Crystals—Textures and Structures*, Gray, G. W., Goodby, J. W. G., Eds.; Leonard Hill: Glasgow, 1984.

(22) (a) Baney, R. H.; Itoh, M.; Sakiara, A.; Suzuki, T. *Chem. Rev.* **1982**, *95*, 199. (b) Agaskar, A. *Colloids Surf.* **1992**, *63*, 131.

(23) Achard, M. F.; S. Lecommandoux, S.; Hardouin, F. *Liq. Cryst.* **1995**, *19*, 581.

as potential precursors to LC ordered organic–inorganic nanocomposites. Although, LC transition temperatures were reduced somewhat, they remain above those considered useful for biologically important applications. However, it should be noted that appending polymer-

izable functionality to these cubes may provide the necessary lowering of the transition temperatures; although it may also affect the formation of LC phases.

CM0100467